Contents lists available at ScienceDirect

CIRP Annals Manufacturing Technology

Journal homepage: www.elsevier.com/locate/cirp

Proposal of 'ImpEC (impact excitation cutting)' for realization of high-flexibility and high-efficiency micro/nano surface texturing

Takehiro Hayasaka[1,*] (2), Pinzhang Sun[1], Hongjin Jung[1], Yudai Mizutani[1], Eiji Shamoto[1] (1)

[1] Graduate School of Engineering, Nagoya University, Furo-cho, Chikusa-ku, Nagoya, Aichi, 464-8603, Japan

In this paper, a novel micro/nano surface texturing method, namely 'ImpEC (impact excitation cutting)', is proposed. To machine micro/nano-textures, vibration cutting and fast tool servo have been utilized. However, the former one is limited to formation of periodical combination of sine waves since the resonance(s) of the cutting tool system is used, and the latter one is limited in terms of efficiency since it has conventionally been utilized within the bandwidth of the servo system, e.g. 3 kHz. Hence, conventional methods cannot realize high flexibility and high efficiency simultaneously. In the proposed ImpEC, the frequencies higher than the resonant frequency are also used, and a series of impacts (pulses) are utilized to diminish the residual vibration. The proposed cutting method can create structures in a short time since the high frequency components are also used, and it can also realize high flexibility since a variety of texturing motions without residual vibrations can be triggered at any timing. The effectiveness of the proposed method is verified both analytically and experimentally.

Cutting; Texturing; Impact excitation cutting

1. Introduction

Micro/nano textures on surfaces of products can enhance characteristics such as hydrophobicity [1], optical functionality [2], and tribological performance [3]. Hence, research interest has focused on the manufacturing of these textures [4]. Especially, ultraprecision diamond cutting has received special focus because of its high precision and high efficiency.

In the literature, a variety of methods have been developed, and many of them have been utilized in practice. The most famous method is the fast tool servo [5-6]. In this method, the frequencies below the resonant frequency of the cutting tool system have been conventionally used to control the trajectory of the tool. Therefore, periodic/aperiodic structures can be machined with a high degree of freedom. Moreover, an ultrafast tool servo was also developed to increase the bandwidth of the system, where a flat gain up to around 3 kHz can be obtained for the closed-loop system [7]. However, this method has a limitation in efficiency since only the frequency components below the resonance are used, and hence the adopted cutting speed is low.

Another method is the vibration cutting [8-9]. To achieve a micron-order vibration amplitude at an ultrasonic frequency, the mechanical resonance of the cutting tool is generally utilized. Due to this nature, the fabricable structures are limited to periodic sine-waves. On the other hand, to increase the flexibility of the machinable micro/nano structures, multi-mode vibration cutting has been developed, where multiple modes of the vibratory cutting tool are utilized so that combination of sine waves can be output [10]. However, the structures are still limited to periodic structures since only the resonant frequency components are utilized.

In summary, it can be said that there is no texturing method which realizes high flexibility and high efficiency simultaneously. In this paper, a novel cutting method named 'ImpEC (impact excitation cutting)' is proposed. In this method, a high frequency range, which includes frequencies higher than the resonance of the cutting tool system, is used so that a high cutting speed can be adopted. In addition, the residual vibration due to the impact excitation of the cutting tool is suppressed by a series of other impacts based on the input shaping method [11]. As a result, a variety of micro/nano structures can be machined at an arbitrary timing, i.e. the flexibility is high. Therefore, the proposed ImpEC can realize high efficiency and high flexibility simultaneously.

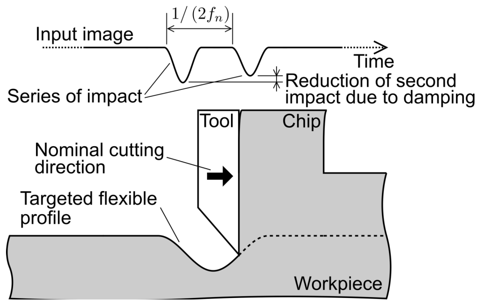

Fig. 1. Schematic of ImpEC.

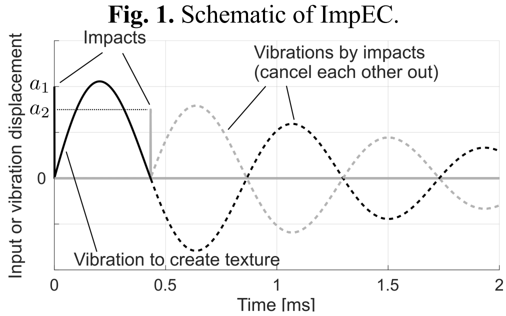

Fig. 2. Texturing and residual vibration suppression in ImpEC.

2. Proposal of ImpEC and analytical investigation

In this chapter, the characteristics of ImpEC is explained in detail. Figure 1 shows a schematic of the proposed method, and

Fig. 2 shows a schematic of how the vibration is suppressed in ImpEC. For simplicity, a single resonant mode for the cutting tool with a resonant frequency of f_n is assumed. In the proposed ImpEC, a series of impacts are utilized to achieve the micro/nano structure and suppress the residual vibration due to other impacts based on the input shaping method [11]. In the beginning, a simple example where the impact is an impulse function is taken into account. Note that electrical impacts are assumed in this research, but force impacts are applied in these simple simulations for simplicity. Firstly, a first impact with a magnitude of a_1 is input at an arbitrary timing. As a result of this impact, vibration occurs mainly at the resonance of the cutting tool, which is shown by a black solid line in Fig. 2. This is because the impact in this example is an impulse. Secondly, another impact is input right after half the resonant time period T_n has passed after the first impact. The vibrations by these two impacts after this half wave length, which are shown by dashed lines, cancel each other out. This is the basic idea of input shaping. T_n and the magnitude of the second impact a_2 can be calculated by the following equations considering the damping of the system where m is the modal mass, k is the modal stiffness coefficient, and ζ is the damping ratio. The values used in this simulation are: $m = 0.4900$ kg, $k = 2.607 \times 10^7$ N/m, and $\zeta = 0.09145$.

$$T_c = \frac{1}{f_c} = 2\pi\sqrt{1-\zeta^2}\sqrt{\frac{m}{k}} \tag{1}$$

$$a_2 = e^{-\frac{\zeta\pi}{\sqrt{1-\zeta^2}}} a_1 \tag{2}$$

The Fourier transform results of the input and the output are shown in Fig. 3. As shown by the result of the input, the resonant frequency component is nearly zero so that the residual vibration due to the resonance is suppressed, and its odd integer multiple components are also nearly zero. On the other hand, other frequency components including frequency components above the resonant frequency compose the input. This is the largest difference between the proposed and conventional surface texturing methods, and the micro/nano structure can be machined flexibly within a short time.

Note that the input can also be prepared using the following method. Assuming the output displacement as $D(j\omega)$ and the frequency response function from input to output as $G(j\omega)$, the input to the cutting tool system $V(j\omega)$ can be calculated as follows.

$$V(j\omega) = D(j\omega)/G(j\omega) \tag{3}$$

Then, the time function of the input $v(t)$ can be obtained by inverse Fourier transforming $V(j\omega)$.

Concerned with the output displacement, it is small since the area of the impact, i.e. area surrounded by the impact and the time axis in Fig. 2, is small in this simple example. To increase the displacement (depth) for applications where microns or tens of microns are needed, this area should also be increased. The shape of the function can be of any kind, e.g. combined step function, sine/cosine-wave function, polynomial function. For example, a cosine-wave function is adopted as shown in Fig. 4. In the same manner as the impulse shape, a second cosine wave with an amplitude of a_2 is input after $T_c/2$ has passed after the first cosine wave. As shown by the resulting displacement, the maximum displacement is tens of microns since the area of the cosine wave is large compared to the impulse. Note that the edge of the structure is round, which is necessary for the surface to obtain specific functionalities, e.g. textures of lubrication surfaces for oil sumps and hydrodynamic pressure, and such flexible structures can be machined efficiently with the proposed method.

Another simulation result is shown where the shape of a targeted cosine-wave structure is constant, and the necessary input

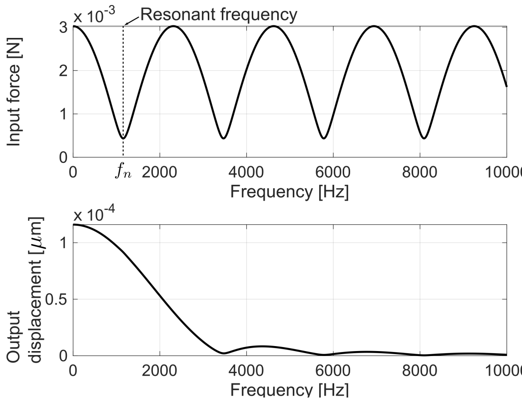

Fig. 3. Fourier transform results of input and output.

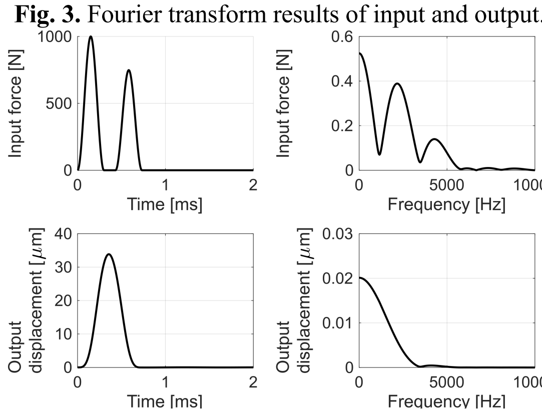

Fig. 4. Example of cosine-wave input using input shaping.

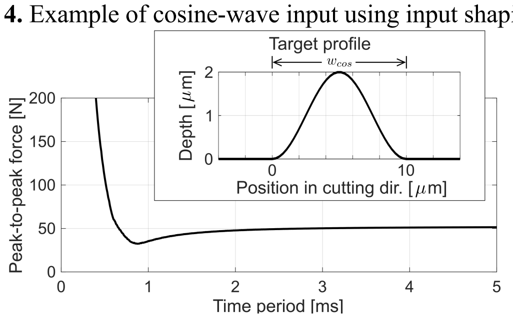

Fig. 5. Target profile and necessary peak-to-peak value.

is calculated with respect to the corresponding time period of the cosine-wave structure, which can be calculated by w_{cos}/v_c where w_{cos} is the length of the structure and v_c is the cutting speed. Hence, a smaller time period means higher efficiency. The necessary peak-to-peak value is calculated and shown in Fig. 5. As shown, the required value is the smallest at the time period of 0.87 ms. This is because the input has a large component at the resonant frequency of the cutting tool. Note that when the time period is large, the flat response part of the transfer function is mainly used, i.e. similar to fast tool servo. For reference, the inputs for the time period of 0.87 ms and 50 ms are shown in Fig. 6. As can be observed, when the time period is 50 ms, the input is nearly proportional to the aimed profile, i.e. frequency components below the resonant frequency are mainly used. On the other hand, the input for the time period of 0.87 ms uses higher frequencies above the resonance and realizes rapid machining. In this example, the adoptable cutting speed in ImpEC is much higher, i.e. the efficiency increases.

Finally, the case where multiple modes of the cutting tool exist is taken into account. A simple impulse function is considered for the input. If the number of modes is assumed as n, the resonant vibrations can be suppressed by 2^n impacts. The input function for an example of two modes is shown in Fig. 7. In addition to the former modal parameters, the following parameters are considered for the second mode: $m_2 = 0.1548$ kg, $k_2 = 5.953 \times 10^7$ N/m, and $\zeta_2 = 0.1212$. In this example, the third impact suppresses the residual vibration of the first mode due to the first impact, and the second impact suppresses the residual vibration of the second mode due to the first impact. The same goes for other relations between impacts.

3. Experimental verification

Experiments are conducted to verify the proposed cutting method. An ultraprecision 5-axis machine tool (ROBONANO α-NMiA, Fanuc Corp.) is utilized for cutting, and a piezoelectric stage (PU1H70F-012U, THK Precision Co., LTD.) is mounted onto it. A photograph of the experimental setup is shown in Fig. 8, and the specifications of the tool/workpiece, the machine tool, and the piezoelectric stage are shown in Table 1. Note that the tool system can be of any kind. The voltage function prepared on a function generator (WF1974, NF Corp.) is input into the piezoelectric stage through an amplifier (HSA4052, NF Corp.) with a gain of 100. The frequency response function G from input voltage to output displacement is measured by inputting sinusoidal waves from 0 to 20 kHz with 20 Hz increments. The displacement of the cutting tool mounted onto the stage is measured by a capacitive sensor (MicroSense 5430 and 5504, ADE Technologies, Inc.). The measured frequency response function is shown in Fig. 9. As shown, the piezoelectric stage itself has multiple peaks around 1 - 3 kHz, and it has a nearly flat response from 0 - 500 Hz. This measured frequency response function is used to calculate the necessary voltage input for the micro/nano structure.

Firstly, three types of structures are targeted to see the output displacement by ImpEC: (1) large cosine-wave structure, (2) small cosine-wave structure, and (3) combined structure composed of cosine-wave part and flat part. The profiles can be expressed as functions of position in the cutting direction x as follows, where f_s ($= 1/48$ for (1) and $1/6$ for (2) and (3)) $[1/(\mu\mathrm{m})]$ is the spatial frequency of the wave and d_a (= 1.6 μm for (1) and 0.2 μm for (2) and (3)) is the amplitude of the wave. Note that f_s and d_a are selected so that interference between the flank face and the workpiece does not occur (maximum instantaneous cutting angle is nearly 6 deg in these examples).

(1) and (2): Large and small cosine-wave structures

$$F_1 = -d_a/2 + d_a/2 \times \cos(2\pi f_s x) \quad (x > 0 \text{ and } x \le f_s) \tag{4}$$

(3) Combination of cosine-wave part and flat part

$$F_2 = \begin{cases} -\dfrac{d_a}{2} + \dfrac{d_a}{2} \times \cos(2\pi f_s x) & \left(x > 0 \text{ and } x \le \dfrac{f_s}{4}\right) \\ -\dfrac{d_a}{2} & \left(x > \dfrac{f_s}{4} \text{ and } x \le \dfrac{3f_s}{4}\right) \\ -\dfrac{d_a}{2} + \dfrac{d_a}{2} \times \cos(2\pi f_s x) & \left(x \ge \dfrac{3f_s}{4} \text{ and } x \le f_s\right) \end{cases} \tag{5}$$

The necessary input voltages to realize these structures are calculated by Eq. (3). The time period of 0.3704 ms for the structures are selected for the experiments. Note that exponential decay windows are applied to the beginning and the ending of the input to exclude unnecessary high frequency components.

Since the frequency response function measured beforehand may change due to nonlinearity like hysteresis, the aimed output profile may not be obtained precisely. In this case, the input voltage profile can be modified as follows. At first, the initially scheduled profile is input into the system, and the output displacement is measured. Next, this output displacement is subtracted from the aimed displacement, and the error is obtained.

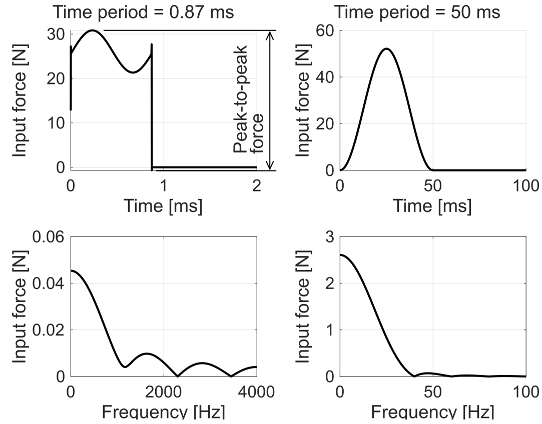

Fig. 6. Inputs for different time periods.

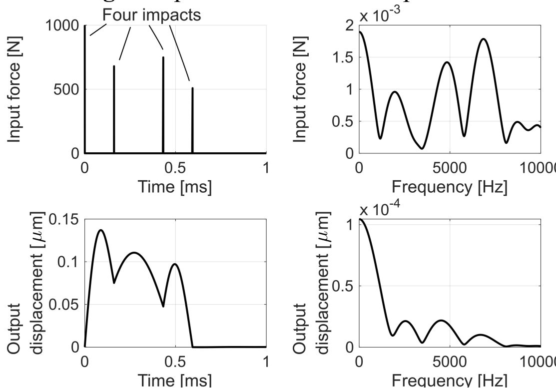

Fig. 7. Residual vibration suppression for multiple modes.

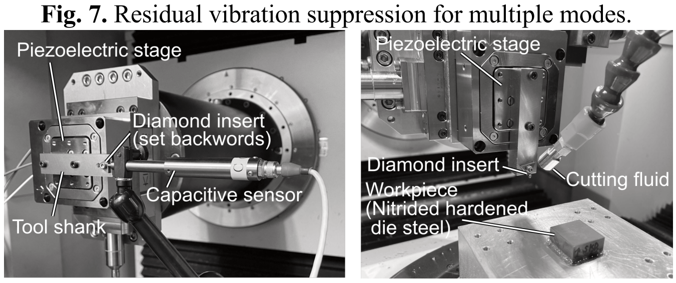

Fig. 8. Photograph of experimental setup: (left) for measurement of vibration and (right) for cutting.

Table 1. Specification of tool/workpiece and equipment.

Workpiece material	Nitrided (EBEP nitriding [11]) hardenened die steel (40CrMoV5)
Tool material	Single crystalline diamond
Nose radius of tool	1 mm
Rake / clearance angle of tool	0 / 10 deg
Cutting speed	0.972 m/min (1 m/min is maximum of machine tool)
Depth of cut	(approximately) 2 μm
Cutting fluid	Insoluble oil
Minimum/maximum applicable voltage to stage	-20 / 150

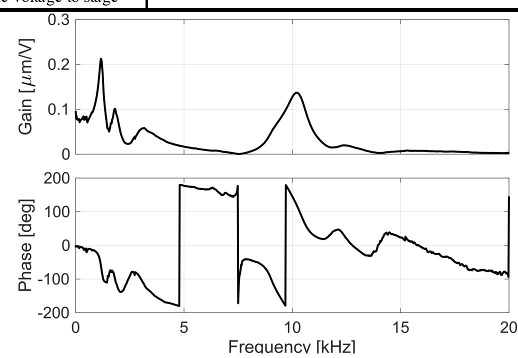

Fig. 9. Measured frequency response function of tool system.

Then, this error is divided by $G(s)$ in the frequency domain, and the additional input corresponding to the error is obtained. Finally, this additional input is added to the initially scheduled input profile, and an improved profile is obtained. This procedure can be repeated arbitrary times for modification. In this experiment, this procedure is repeated 7, 1, and 4 time/s for (1), (2), and (3), respectively. The measured/targeted profiles and an example of the modified input profile are shown in Figs. 10 and 11, respectively. Note that the displacement is measured 500 times, and these data are averaged so that the noise irrelative to the measurement is nearly eliminated. As shown, the measured and targeted profiles agree well. It can also be observed that frequency components higher than the resonance are used in ImpEC.

Secondly, cutting is conducted based on structure (2). In this experiment, a profile shown in Fig. 12 is utilized. Each structure is that of structure (2), and its corresponding input is repeated within the time width of 4 ms in an aperiodic manner. This aperiodic profile is repeated during the cutting. Nitrided (EBEP nitriding [12]) hardened die steel is selected as the workpiece, and groove cutting is conducted with a depth of cut of approximately 2 µm. The profile and photograph of the machined structure along the cutting direction measured by a 3D optical profiler (NewView 9000, Zygo Corp.) is shown in Fig. 13. For reference, a machined single texture (planing at pick feed of 20 µm and depth of cut of 6 µm) is also shown. As can be observed, sub-micron order textures are machined against hardened die steel. Note that the roughness due to cutting is relatively large since the size of the texture is small. This can be made large by adopting higher cutting speeds and utilization of special tools. It can also be observed that the residual vibration is extremely small, and aperiodic textures can be machined. These results prove the validity of the proposed method.

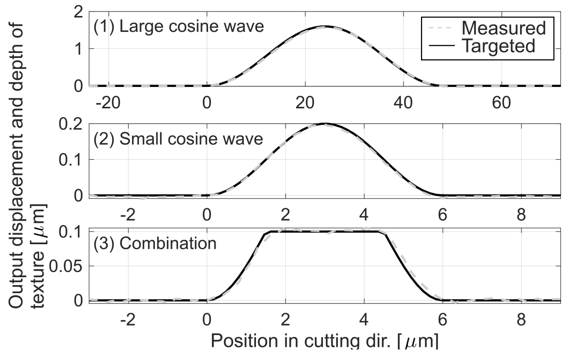

Fig. 10. Comparison of measured and targeted single profiles.

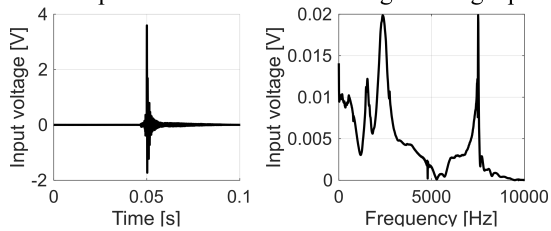

Fig. 11. Modified input voltage for small cosine wave.

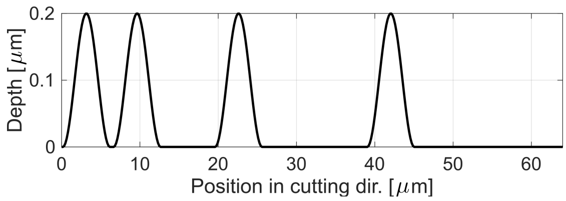

Fig. 12. Targeted profile for aperiodic textures based on small cosine-wave structure.

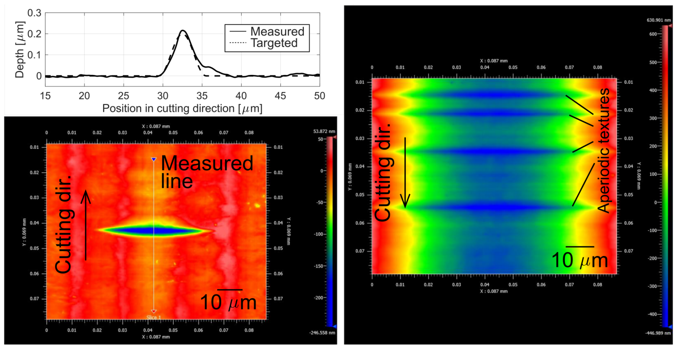

Fig. 13. Machined single/aperiodic textures and measured surface profile.

6. Conclusion

A novel texturing method named ImpEC has been proposed in this paper. In the proposed method, a series of impacts are prepared to generate the texture and suppress the residual vibration. Compared to fast tool servo, where the frequency components below the resonance are utilized, the proposed method utilizes components above the resonance also, which means that higher efficiency can be achieved. Compared to vibration cutting, aperiodic textures can be machined since residual vibration is suppressed, which means that higher flexibility can be achieved. Analyses and experiments have been conducted to verify the proposed method. In the experiments, nitrided hardened die steel has been cut applying ImpEC, and sub-micron order aperiodic textures have been machined. These results prove that high flexibility and high efficiency can be realized simultaneously by using ImpEC.

Acknowledgments

The research is supported by the Program for Building Regional Innovation Ecosystem “Aichi Innovation Ecosystem Project for Next-Generation Automobile” from the Ministry of Education, Culture, Sports, Science and Technology of Japan. In addition, the authors would like to express their sincere thanks to FANUC Corp. for their help to conduct the present research.

References

[1] Callies M, Chen Y, Marty F, Pepin A, Quere D (2005) Microfabricated textured surfaces for super-hydrophobicity investigations. *Microelectronic Engg.* 78-79: 100-105.

[2] Sun L, Jin S, Cen S (2009) Free-form microlens for illumination applications. *Applied Optics* 48(29): 5520-5527.

[3] Pettersson U, Jacobson S (2003) Influence of surface texture on boundary lubricated sliding contacts. *Tribology Int.* 36: 857-864.

[4] Brinksmeier E, Karpuschewski B, Yan J, Schonemann L (2020) Manufacturing of multiscale structured surfaces. *CIRP Annals – Manuf. Tech.* 69: 717-739.

[5] Patterson S R, Magrab E B (1985) Design and testing of a fast tool servo for diamond turning. *Precision Engg.* 7(3): 123-128.

[6] Rakuff S, Cuttino J F (2009) Design and testing of a long-range, precision fast tool servo system for diamond turning. *Precision Engg.* 33: 18-25.

[7] Lu X D, Trumper D L (2005) Ultrafast Tool Servos for Diamond Turning. *CIRP Annals* 54(1): 383-388.

[8] Kumabe J (1983) Precision High Speed Vibration Cutting (in Japanese). *Japan Patent Office*: 58-143901.

[9] Guo P, Ehmann K N (2013) Development of a tertiary motion generator for elliptical vibration texturing. *Precision Engg.* 37: 364-371.

[10] Jung H et al. (2019) Proposal of Ultrasonic Multi-Mode Vibration Cutting for High-Efficiency Surface Texturing. *Int. Symp. on Precision Engg. and Sustainable Manuf.* Da Nang, Vietnam.

[11] Singer N C, Seering W P (1990) Preshaping Command Inputs to Reduce System Vibration. *J. Dyn. Sys., Meas., Control* 112(1): 76-82.

[12] Saito H, Jung H, Shamoto E, Hara Y, Hara T (2020) Suppression of tool damage in ultraprecision diamond machining of stainless steel by applying electron-beam-excited plasma nitriding. *Precision Engg.* 63:126-136.